JACS
JOURNAL OF THE AMERICAN CHEMICAL SOCIETY

ARTICLE

pubs.acs.org/JACS

Isolation and Crystallographic Identification of Four Isomers of Sm@C_{90}

Hua Yang,[‡,∥] Hongxiao Jin,[‡] Hongyu Zhen,[∥] Zhimin Wang,[∥] Ziyang Liu,[*,‡,∥] Christine M. Beavers,[§] Brandon Q. Mercado,[†] Marilyn M. Olmstead,[*,†] and Alan L. Balch[*,†]

[‡]College of Materials Science and Engineering, China Jiliang University, Hangzhou 310018, China

[∥]State Key Laboratory of Modern Optical Instrumentation and Department of Chemistry, Zhejiang University, Hangzhou 310027, China

[§]Advanced Light Source, Lawrence Berkeley National Laboratory, One Cyclotron Road, Berkeley, California 94720, United States

[†]Department of Chemistry, University of California, One Shields Avenue, Davis, California 95616, United States

Supporting Information

ABSTRACT: Four isomers with the composition SmC_{90} were obtained from carbon soot produced by electric arc vaporization of carbon rods doped with Sm_2O_3. These were labeled Sm@C_{90}-(I), Sm@C_{90}(II), Sm@C_{90}(III), and Sm@C_{90}(IV) in order of their elution times during chromatography on a Buckyprep column with toluene as the eluent. Analysis of the structures by single-crystal X-ray diffraction on cocrystals formed with Ni(octaethylporphyrin) reveals the identities of the individual isomers as follows: I, Sm@C_2(40)-C_{90}; II, Sm@C_2(42)-C_{90}; III, Sm@C_{2v}(46)-C_{90} and IV, Sm@C_2(45)-C_{90}. This is the most extensive series of isomers of any endohedral fullerene to have their individual structures determined by single-crystal X-ray diffraction. The cage structures of these four isomers can be related pairwise to one another in a formal sense through sequential Stone−Wales transformations.

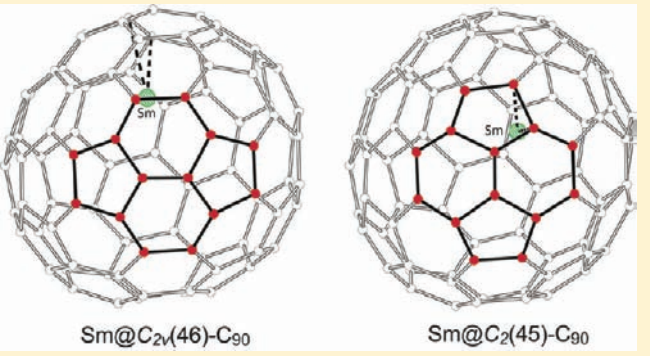

INTRODUCTION

Endohedral fullerenes consist of closed carbon cages that surround an atom, atomic cluster, or molecule.[1,2] The simplest of these are the endohedral fullerenes that contain only a single atom. A rather diverse array of individual atoms can be trapped inside fullerenes. The relatively inert nobel gas atoms He, Ne, Kr, Ar, and Xe have each been trapped inside C_{60}.[3] For example, He@C_{60} is formed along with C_{60} during the preparation of fullerenes using the classical electrical arc method that employs a low-pressure helium atmosphere.[4] However, only one out of every million C_{60} molecules produced this way contains a helium atom. ^{3}He and ^{129}Xe are spin 1/2 nuclei whose NMR spectra can be observed. Thus, the ^{3}He and ^{129}Xe NMR spectra of ^{3}He@C_{60} and ^{129}Xe@C_{60} have been used to monitor the reactivity of the outside of these cages.[5] At the other end of the reactivity scale, atoms of nitrogen or phosphorus have also been encapsulated in C_{60}. Atomic N and P are highly reactive atoms that few chemists have directly encountered, yet N@C_{60} and P@C_{60} appear to have considerable stability, while retaining spectroscopic features similar to those of these gas-phase atoms themselves.[6,7] The shielded environment of the $^4S_{3/2}$ electronic state of the nitrogen atom in N@C_{60} gives it a long spin relaxation time. As a result, the use of N@C_{60} as a component in solid-state quantum computers has been suggested.[8]

By far the most numerous endohedral fullerenes are those that contain electropositive metal atoms: alkali, alkaline earth, and lanthanide atoms. Indeed, the first endohedral to be observed, La@C_{60},[9] belongs to this class, as does the first soluble endohedral to be isolated, La@C_{82}.[10] Subsequently, an intriguing array of monometallic endohedral fullerenes have been prepared and isolated. Since it is electropositive metals that are incorporated into the carbon cages and these carbon cages are readily reduced, there is charge transfer between the metal atom and the cage. Thus, the interaction between the interior atom and the cage is much greater for metal-containing endohedral fullerenes than is the case for molecules like He@C_{60} and N@C_{60}. For endohedral fullerenes containing lanthanide ions, two classes of molecules have been identified. For those containing Sc, Y La, Ce, Pr, Nd, Gd, Tb, Dy, Ho, Er, and Lu, three electrons are transferred from the metal to the cage. However, for those involving Sm, Eu, Tm, and Yb, only two electrons are transferred to the cage, as is also the case for endohedrals involving alkaline earth atoms.

Received: December 20, 2010
Published: March 31, 2011

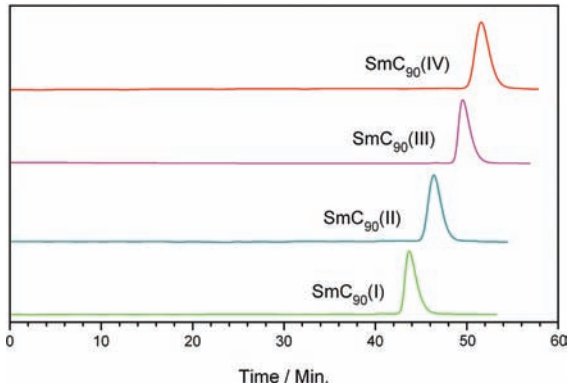

Figure 1. Chromatograms of the isolated Sm@C_{90} isomers on a Buckyprep column with toluene as the eluent. The HPLC conditions are flow rate of 4.0 mL/min and detection wavelength of 450 nm.

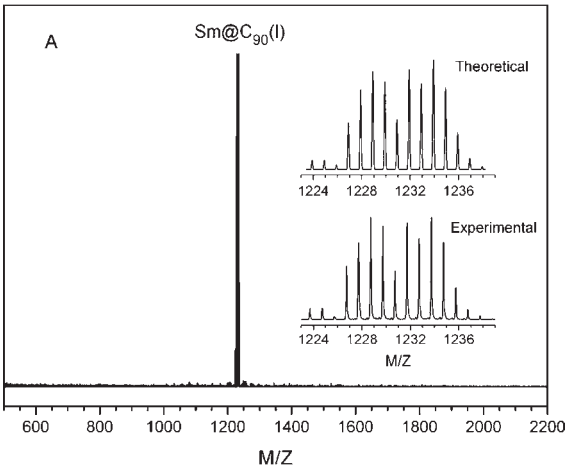

Figure 2. LD-TOF mass spectra of the purified sample of Sm@C_{90}(I). The insets show expansions of the experimental and theoretical isotope distributions. The experimental mass spectra of the other three isomers, which appear in the Supporting Information, are nearly identical and differ only in the signal-to-noise ratio in each spectrum.

For endohedral fullerenes containing a single metal atom, a wide range of cage sizes have been encountered, and for each cage size there is the potential to form cage isomers. For example, numerous endohedral fullerenes containing a single samarium atom have been isolated from the carbon soot that is produced by vaporizing samarium oxide-doped carbon rods in a conventional fullerene generator.[11−13] These endohedral fullerenes include Sm@C_{74}, Sm@C_{76} (two isomers), Sm@C_{78}, Sm@C_{80}, Sm@C_{82} (four isomers), Sm@C_{84} (three isomers), Sm@C_{86}, Sm@C_{88} (three isomers), Sm@C_{90} (three isomers), Sm@C_{92} (two isomers), Sm@C_{94} (three isomers), and Sm@C_{96}. These samarium-containing endohedrals have been characterized by chromatographic retention times, mass spectrometry, UV−vis−NIR spectroscopy, and cyclic voltammetry. Examination of those with cages smaller than C_{86} by electron energy-loss spectroscopy (EELS) has indicated that the oxidation state of the samarium is +2.[14,15] However, definitive structural information is not yet available for any of these 25 compounds. Here, we report the isolation of four isomers of Sm@C_{90} in quantities that allowed us to obtain crystals suitable for single-crystal X-ray diffraction studies on each isomer.

For C_{90} there are 46 isomers that obey the isolated pentagon rule (IPR).[16] The IPR requires that each of the 12 pentagons of a fullerene is surrounded by 5 hexagons. Recently, we reported the isolation and structural characterization of D_{5h}(1)-C_{90}, a remarkable and highly symmetric fullerene with a capped nanotubular structure that was formed utilizing a conventional electric arc with graphite rods doped with Sm_2O_3.[17] Since D_{5h}(1)-C_{90} had not been reported in other preparations of C_{90} isomers that used undoped graphite rods,[18] it appears that the presence of Sm_2O_3 altered the distribution of isomers that were produced. Crystallographic studies of two other C_{90} isomers, which were formed along with D_{5h}(1)-C_{90} from doped graphite rods Sm_2O_3, have shown that, unlike most fullerenes that are highly symmetrical, they have only C_1 symmetry.[19] These two isomers, C_1(30)-C_{90} and C_1(32)-C_{90}, are very similar in their structures and are related by a single Stone−Wales transformation. In contrast, the highly symmetric D_{5h} isomer cannot be converted into any other C_{90} isomer by such a transformation.

RESULTS

Isolation of Four Isomers of Sm@C_{90}. Carbon soot containing the samarium endohedral fullerenes along with empty cage fullerenes was obtained by vaporizing a graphite rod filled with Sm_2O_3 and graphite powder in an electric arc as outlined earlier.[17,20,21] The soot was extracted with *o*-dichlorobenzene and concentrated. This soluble extract was subjected to a four-stage, high-pressure liquid chromatographic (HPLC) isolation process that resulted in the separation of four individual isomers of Sm@C_{90}. The same procedure also afforded three isomers of empty cage C_{90}.[17,19] The Sm@C_{90} isomers are labeled Sm@C_{90}(I), Sm@C_{90}(II), Sm@C_{90}(III), and Sm@C_{90}(IV) in order of their elution times during chromatography on a Buckyprep column with toluene as the eluent. Figure 1 shows the chromatograms of the four isomers that were isolated. The relative abundances of the isolated isomers are 7 (I):20 (II):1 (III):8 (IV). Figure 2 shows the laser desorption time-of-flight (LD-TOF) mass spectrum of Sm@C_{90}(I) along with the spectrum computed on the basis of isotope abundances. The corresponding spectra (see the Supporting Information) for the other three isomers are similar. Variations in the signal-to-noise ratio are the principal differences between them.

The UV−vis−NIR absorption spectra of the individual isomers are shown in Figure 3, along with pictures of the colored solutions of the isomers. Previously, Liu et al. reported the isolation of three isomers (here labeled I^L, II^L, and III^L) of Sm@C_{90}.[13] Comparison of their UV−vis−NIR absorption spectra with the data presented in Figure 3 shows that our isomers Sm@C_{90}(I) and Sm@C_{90}(II) correspond to their isomers Sm@C_{90}(I^L) and Sm@C_{90}(II^L). The spectrum we report for Sm@C_{90}(III) is unlike any of the spectra Liu et al. reported, and hence this is a new isomer. The yield of Sm@C_{90}(III) is the lowest of these isomers, and so it is not surprising that its presence could have been overlooked in the earlier study. The spectrum we obtained for Sm@C_{90}(IV) corresponds to the spectrum Liu et al. reported for their isomer Sm@C_{90}(III^L).

The four Sm@C_{90} isomers display different UV−vis−NIR absorption spectra, while the two green ones, Sm@C_{90}(I) and Sm@C_{90}(II), have similar strong absorption bands. The two orange isomers, Sm@C_{90}(III) and Sm@C_{90}(IV), also show some similarity, but Sm@C_{90}(IV) shows a distinctly low energy onset of 1530 nm.

Single-Crystal X-ray Diffraction Studies of the Four Isomers. Analysis of the structures reveals the identities of the individual

dx.doi.org/10.1021/ja111465n |*J. Am. Chem. Soc.* 2011, 133, 6299–6306

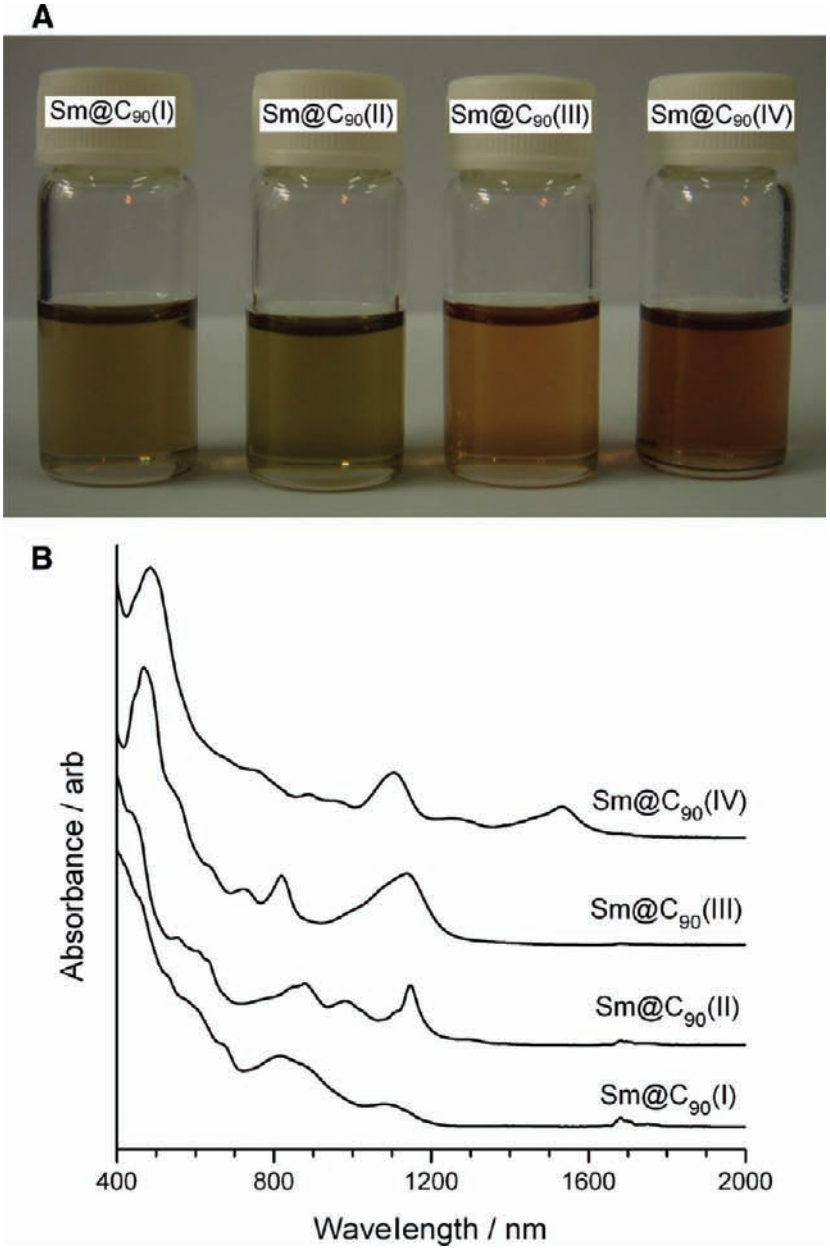

Figure 3. (A) Photograph of isolated Sm@C_{90} isomers. (B) UV−vis−NIR absorption spectra of the isolated Sm@C_{90} isomers dissolved in carbon disulfide.

isomers: I, Sm@C_2(40)-C_{90}; II, Sm@C_2(42)-C_{90}; III, Sm@C_{2v}-(46)-C_{90}; and IV, Sm@C_2(45)-C_{90}. All of the structures show some degree of disorder in the position of the fullerene cage. Details of the disorder are given in the Experimental Section.

Figure 4 shows the structure of the endohedral fullerene and its relationship to the nickel porphyrin in the crystal of Sm@C_{2v}-(46)-C_{90}·NiOEP·2toluene. This is the structure in which the samarium atom inside the fullerene is the most localized, with 0.58 fractional occupancy at the site shown. Additionally, this crystal contains the most symmetric carbon cage of the four isomers. As shown in Figure 4, the samarium atom resides on the crystallographic 2/*m* axis with distances Sm1···C89, 2.598(4) Å and Sm1···C90, 2.541(5) Å to a 6:6 ring junction.

Drawings of the carbon cages for all four isomers are displayed in Figure 5. In these drawings the two-fold axis of each cage is positioned perpendicularly to the plane of the page (or screen) and runs through the middle of the central hexagon. A notable feature of each cage is the existence of a band of 11 contiguous hexagons that encircles the cage and is aligned horizontally in Figure 5. For the three isomers with C_2 symmetry, the presence of a crystallographic mirror plane ensures that each crystal contains a racemate.

Figure 6 shows the distribution of metal atoms sites inside the most prevalent orientation of the fullerene cages. Each cage is seen from a perspective that places the ring of 11 contiguous hexagons perpendicular to the picture plane. The metal atoms' positions are generally distributed along the bands of hexagons. Similar arrangements of multiple metal atom sites along bands of contiguous hexagons have been seen previously in Er_2@C_s(6)-C_{82},[22] Er_2@C_{3v}(8)-C_{82},[23] and $Sc_2(\mu_2\text{-O})$@C_s(6)-C_{82}.[24] However,

dx.doi.org/10.1021/ja111465n |*J. Am. Chem. Soc.* 2011, 133, 6299–6306

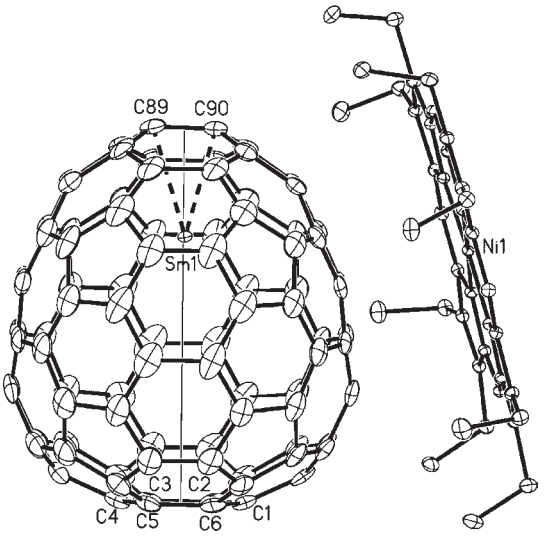

Figure 4. Interaction between the fullerene and porphyrin in Sm@C_{2v}-(46)-C_{90}·NiOEP·2toluene with 30% thermal elipsoids. Only the major sites for the fullerene at 0.88 fractional occupancy and the samarium atom with 0.58 fractional occupancy are shown. For clarity, the toluene molecules are not shown. The vertical line shows the location of the non-crystallographic two-fold axis of the carbon cage.

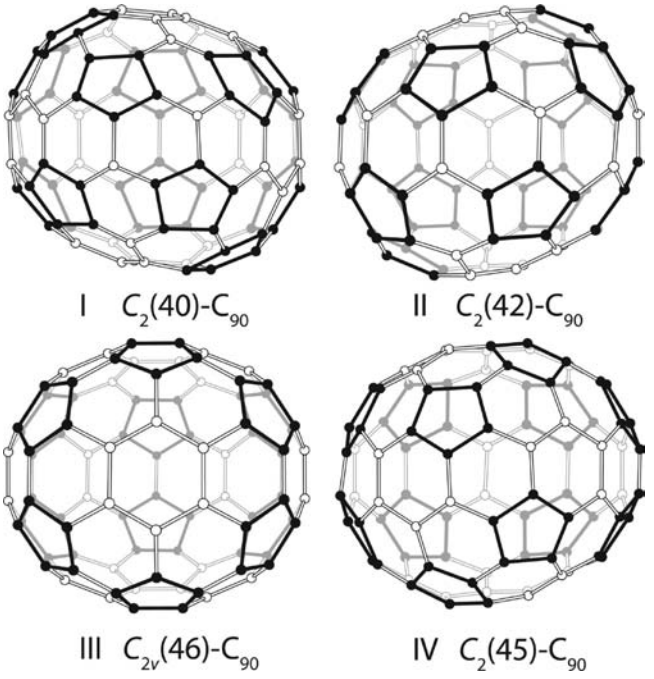

Figure 5. Drawings showing the carbon cages for the isomers: I, Sm@C_2(40)-C_{90}; II, Sm@C_2(42)-C_{90}; III, Sm@C_{2v}(46)-C_{90}; and IV, Sm@C_2(45)-C_{90}. The pentagons are highlighted in black. In each drawing the two-fold axis of the fullerene lies perpendicular to the picture plane and passes through the central hexagon and the vertical bond immediately behind that hexagon. Only one, arbitrarily selected enantiomer of each C_2 isomer is shown.

it should be noted that there are alternate orientations of the cages in each crystal. Unfortunately, there is no way to correlate the positions of the metal atoms that we have identified with any specific cage oreintation. Since there are several cage orientations

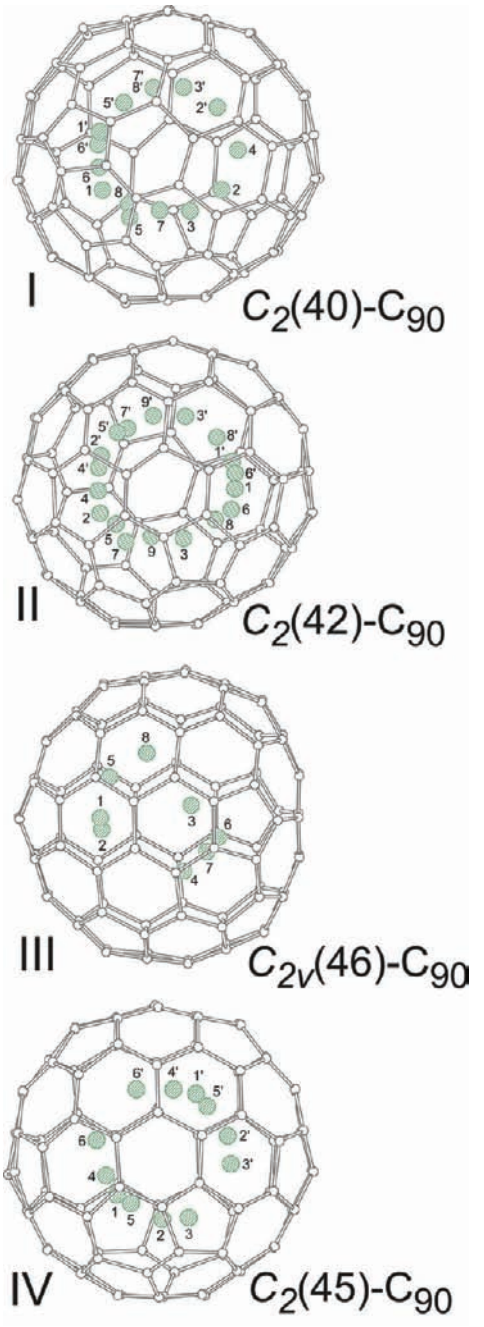

Figure 6. Drawings showing the locations of the various partially occupied sites for the samarium atom in I, Sm@C_2(40)-C_{90}; II, Sm@C_2(42)-C_{90}; III, Sm@C_{2v}(46)-C_{90}; and IV, Sm@C_2(45)-C_{90}. The fullerene cages are oriented so that the viewer is looking down the center of the ring of 11 contiguous hexagons. The picture plane bisects that ring.

in the crystal of each isomer, it is possible that fewer metal atom positions are associated with particular cage orientations than those shown in Figure 6. Nevertheless, it appears that the samarium atoms occupy multiple positions within each of the different isomers. At this stage there is no way to obtain further information about the specifics of metal atom placement from the crystallographic data.

The four isomers of Sm@C_{90} are all inter-related by the simple reorientation of a pair of carbon atoms in a pyracylene unit, which

dx.doi.org/10.1021/ja111465n |*J. Am. Chem. Soc.* 2011, 133, 6299–6306

Scheme 1. Stone−Wales Transformation and Paths for Stone−Wales Interconversion of Sm@C_{90} Isomers

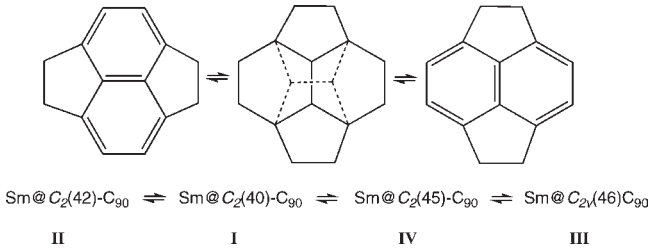

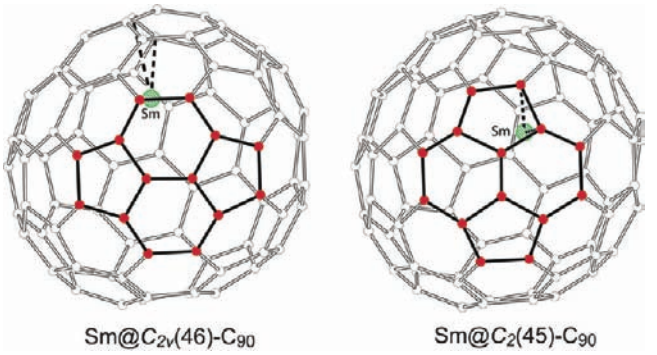

Figure 7. Views of Sm@C_{2v}(46)-C_{90} and Sm@C_2(45)-C_{90} from a perspective that shows that the carbon cages of the two isomers are related by a single Stone−Wales transformation. The Stone−Wales patch is highlighted with solid black bonds and red atoms. Note that all of the gray atoms in each isomer have similar locations and connectivities.

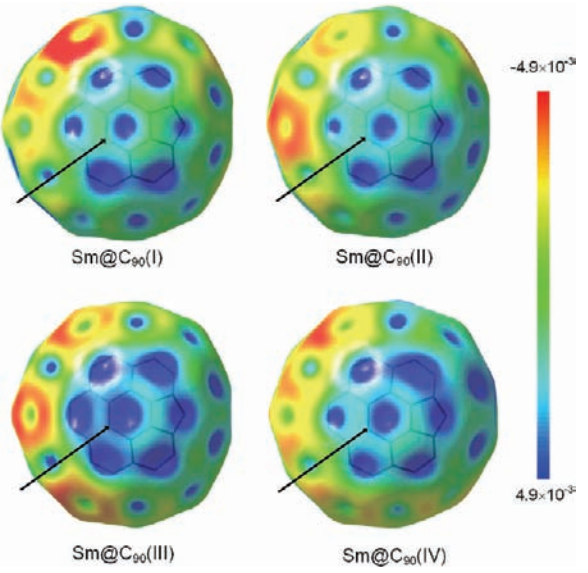

Figure 8. Plots of electrostatic potential in terms of total electron density (0.001 e/Bohr^3) mapped on the isosurface facing the Ni(OEP) for the four isomers of Sm@C_{90}. Two-dimensional projections of the bonds onto the plots are also shown for clarity. The lines indicate the carbon atoms nearest the nickel ion.

is known as the Stone−Wales transformation[25] and shown in Scheme 1. This scheme also demonstrates that each of the four Sm@C_{90} isomers may be converted into another isomer through a single Stone−Wales transformation. As an example, Figure 7 shows the structures of a representative pair: Sm@C_{2v}(46)-C_{90} and Sm@C_2(45)-C_{90}. In this drawing the critical pyracylene patches face the viewer and are highlighted with red atoms and solid black connectors (bonds). Notice that while a pair of carbon atoms within this patch rotates by 90°, the remaining carbon atoms in the cage retain their locations, which are nearly identical in the two isomers. Similar relationships exist between the structures of Sm@C_2(40)-C_{90} and Sm@C_2(42)-C_{90} and between the structures of Sm@C_2(40)-C_{90} and Sm@C_2(45)-C_{90}.

Figure 8 shows the electrostatic potential on the surfaces of the Sm@C_{90} isomers that face the Ni(OEP) molecule in the crystal. The lines in the drawing indicate the carbon atoms that are closest to the Ni atom in Ni(OEP). It is remarkable that a similar patch on the surface of each fullerene interacts with the porphyrin. In each case it is an electron-poor region of the fullerene that faces the porphyrin, which presents an electron-rich region near the nitrogen atoms of the porphyrin.[17] Similar electron-poor regions of other fullerenes have been found in contact with Ni(OEP).[17,19,26]

Computational Studies of the Relative Stabilities of the Sm@C_{90} Isomers. Computations were performed at the B3LYP level with 3-21g(d) basis set to compare the relative stabilities of the Sm@C_{90} isomers. The optimized cage structures obtained from these computations agree with the crystallographically determined structures. Table 1 shows the relative energy, HOMO−LUMO gap, and relative abundance of the four isomers in the order of relative energy from the lowest to the highest. The relative energies and the HOMO−LUMO gaps follow similar trends. The data indicate that Sm@C_2(42)-C_{90}, which is the most abundant of the four isomers, has the lowest relative energy along with the largest HOMO−LUMO gap, and in general the relative abundance of the isomers correlates with the computed relative energies, which have omitted consideration of entropic factors that become significant at the high temperature at which these endohedrals are formed.[27] The low band gap computed for Sm@C_2(45)-C_{90} is consistent with the observed low energy onset of absorption seen in the UV−vis−NIR spectrum.

DISCUSSION

Prior work on the identification of isomers of monometallic endohedral fullerenes has focused largely on molecules with cage sizes in the range C_{80}−C_{84}. ^{13}C NMR studies of diamagnetic endohedral fullerenes have been able to identify the cage symmetry and, when coupled with computational simulation of spectra, have been utilized to identify specific cage isomers. Thus, for example, with metal ions that transfer two electrons to the fullerene cage, four isomers of Ca@C_{82}, where there are nine possible isomers that obey the isolated pentagon rule, have been shown to have C_s, C_{3v}, C_2, and C_{2v} symmetry.[28] Similarly, the one isomer of Yb@C_{80} so far observed has been identified as Yb@C_{3v}(3)-C_{80}.[29] The three isomers of Yb@C_{82} have been shown be Yb@C_s(6)-C_{82}, Yb@C_2(5)-C_{82}, and Yb@C_{2v}(9)-C_{82},[29] and three of the four known isomers of Yb@C_{84} have been characterized as Yb@C_2(13)-C_{84}, Yb@C_1(12)-C_{84}, and Yb@C_2(11)-C_{84}.[29] As the cage size of fullerenes increases, it becomes more difficult to determine the specific isomers involved because the number of possible isomers increases. For example, while C_{80} has seven cages that obey the isolated pentagon rule, C_{90} has 46 such isomers.

Our work has identified the geometric structures of the four most abundant forms of Sm@C_{90}: I, Sm@C_2(40)-C_{90}; II, Sm@C_2(42)-

Table 1. Results from DFT Computations[a]

isomer	relative energy, kcal/mol	HOMO−LUMO gap, eV	relative abundance
II, green, Sm@C_2(42)-C_{90}	0.000	1.731	20
IV, orange, Sm@C_2(45)-C_{90}	2.633	1.382	8
I, green, Sm@C_2(40)-C_{90}	3.253	1.546	7
III, orange, Sm@C_{2v}(46)-C_{90}	4.730	1.545	1

[a] DFT function, B3LYP; basis set, 3-21g for C, CEP-31g for Sm.

Table 2. Crystal Data and Data Collection Parameters

	Sm@C_2(40)-C_{90}·Ni(OEP)·2chlorobenzene	Sm@C_2(42)-C_{90}·Ni(OEP)·2toluene	Sm@C_2(46)-C_{90}·Ni(OEP)·2toluene	Sm@C_2(45)-C_{90}·Ni(OEP)·2toluene
isomer	I	II	III	IV
formula	$C_{138}H_{54}Cl_2N_4NiSm$	$C_{140}H_{60}N_4NiSm$	$C_{140}H_{60}N_4NiSm$	$C_{140}H_{60}N_4NiSm$
fw	2047.81	2006.98	2006.98	2006.98
color, Habit	black parallelepiped	black parallelepiped	black parallelepiped	black parallelepiped
crystal system	monoclinic	monoclinic	monoclinic	monoclinic
space group	*C*2/*m*	*C*2/*m*	*I*2/*a*	*C*2/*m*
a, Å	25.283(2)	25.274(7)	25.5939(13)	25.5045(7)
b, Å	15.3956(12)	15.378(4)	15.2087(6)	15.3357(4)
c, Å	20.7739(17)	20.749(6)	41.538(2)	20.6732(6)
β, deg	94.899(4)	94.921(3)	95.150(3)	95.399(2)
V, Å^3	8056.7(11)	8035(4)	16103.3(14)	8050.1(4)
Z	4	4	8	4
radiation (λ, Å)	synchrotron (0.77490)	synchrotron (0.68890)	sealed tube (0.71073)	sealed tube (0.71073)
unique data	10 693 [*R*(int) = 0.045]	12 317 *R*(int) = 0.037]	25 610 [*R*(int) = 0.0327]	12 158 [*R*(int) = 0.025]
obsd ($I > 2\sigma(I)$) data	10 255	11 258	21 012	9 917
*R*1[a] (obsd data)	0.0660	0.0671	0.0775	0.0526
w*R*2[b] (all data)	0.1824	0.1868	0.2336	0.1520

[a] For data with $I > 2\sigma(I)$. $R1 = (\Sigma||F_o| - |F_c||)/(\Sigma|F_o|)$. [b] For all data. $wR2 = ((\Sigma[w(F_o^2 - F_c^2)^2])/(\Sigma[w(F_o^2)^2]))^{1/2}$.

C_{90}; III, Sm@C_{2v}(46)-C_{90}; and IV, Sm@C_2(45)-C_{90}. This is the most extensive series of isomers of any endohedral fullerene to have their individual structures determined by single-crystal X-ray diffraction. The cage structures of these four isomers are related pairwise to one another through the Stone−Wales transformation as shown in Scheme 1. It may be that these isomers interconvert through such Stone−Wales transformations at the temperature at which they are being formed in the electric arc process of fullerene generation. Notice that the four isomers of Sm@C_{90} that have been isolated all have cages that appear near the end of the list of C_{90} isomers produced by Fowler and Manolopoulous.[16] These are the isomers with the largest separations between the pentagonal rings, which are the sites where negative charge resides in the anionic fullerene cages.[30]

Several isomeric fullerenes with the C_{90} cage are now known to be stable and are structurally characterized. The process that produced the four isomers of Sm@C_{90} whose structures are reported here also produced three isomers of empty-cage C_{90}: D_{5h}(1)-C_{90}, C_1(30)-C_{90}, and C_1(32)-C_{90}.[17,19] These three empty-cage fullerenes have been crystallographically characterized. Prior to that, Achiba et al. utilized ^{13}C NMR spectroscopy to show that a sample of C_{90} isomers produced from undoped carbon rods contained five C_{90} isomers: one with C_{2v} symmetry, three with C_2 symmetry, and one with C_1 symmetry.[18] A number of structural studies have examined the products of functionalization of empty-cage C_{90}. Two trifluoromethyl adducts of C_{90}, with the composition $C_{90}(CF_3)_{12}$, were obtained by addition of CF_3I to a mixture of higher fullerenes. The ^{19}F NMR spectra of these two adducts showed that the fullerene cage in each had only C_1 symmetry, but there are 16 isomers of C_{90} with C_1 symmetry.[31] One adduct was shown to involve the C_1(32)-C_{90} cage, but the specific identity of the second isomer with C_1 symmetry was unclear. Treatment of a mixture of higher fullerenes with $SbCl_5$ produced a crystal that contained a mixture of two isomers with the composition $C_{90}Cl_{32}$.[32] An X-ray diffraction study revealed that one isomer was formed from the C_{2v}(46)-C_{90} cage, while the other was derived from the C_s(34)-C_{90} cage.

As shown in Figure 6, the samarium ion in each these four isomers shows significant disorder but does tend to prefer locations along a band of 11 contiguous hexagons. This sort of behavior is not necessarily a property of large carbon cages containing only a single metal atom. The structures of Tm@C_{3v}-C_{94} and Ca@C_{3v}-C_{94}, which involve a larger cage size, both show the metal ions confined to only three, nearly equivalent sites along the C_3 axis.[33]

EXPERIMENTAL SECTION

Synthesis of the Four Sm@C_{90} Isomers. An 8 × 150 mm graphite rod filled with Sm_2O_3 and graphite powder (Sm:C atomic ratio 1:40) was vaporized as the anode in DC arc discharge under optimized conditions. The raw soot was sonicated in *o*-dichlorobenzene for 8 h and then filtered with the aid of a vacuum. After removal of the solvent with a

dx.doi.org/10.1021/ja111465n |*J. Am. Chem. Soc.* 2011, 133, 6299–6306

rotary evaporator, chlorobenzene was added to redissolve the dry extract. The resulting solution was subjected to a four-stage HPLC isolation process without recycling. Chromatographic details are given in the Supporting Information.

The purity and composition of the samples of isomers of Sm@C_{90} were verified by laser desorption time-of-flight mass spectrometry (LD-TOF-MS). Ultraviolet−visible−near-infrared (UV−vis−NIR) spectra were obtained through the use of a UV-4100 spectrophotometer (Hitachi High-Technologies Corp.) with samples dissolved in carbon disulfide.

Crystal Growth. Co-crystals of the Sm@C_{90} isomers and Ni^{II}(OEP) were obtained by layering a nearly saturated solution of the endohedral in toluene or chlorobenzene over a red toluene solution of Ni^{II}(OEP) in a glass tube. Over a 14-day period, the two solutions diffused together, and black crystals formed.

Crystal Structure Determinations. Black crystals of Sm@C_2(46)-C_{90}·Ni(OEP)·2toluene and Sm@C_2(45)-C_{90}·Ni(OEP)·2toluene were mounted in the nitrogen cold stream provided by a Cryo Industries low-temperature apparatus on the goniometer head of a Bruker SMART diffractometer equipped with an ApexII CCD detector. Data were collected with the use of Mo Kα radiation (λ = 0.71073 Å). Crystal data are given in Table 2. Black crystals of Sm@C_2(40)-C_{90}·Ni(OEP)·2chlorobenzene were mounted in the 100(2) K nitrogen cold stream provided by an Oxford Cryostream low-temperature apparatus on the goniometer head of a Bruker D8 diffractometer equipped with an ApexII CCD detector, on beamline 11.3.1 at the Advanced Light Source in Berkeley, CA. Diffraction data were collected using synchrotron radiation monochromated with silicon(111) to a wavelength of 0.77490 Å.

Black crystals of Sm@C_2(42)-C_{90}·Ni(OEP)·2toluene were mounted in the 120(2) K nitrogen cold stream provided by an Oxford Cryostream low-temperature apparatus on the goniometer head of a Rigaku Saturn724+ diffractometer, on beamline I19 at the Diamond Light Source Ltd. in Oxfordshire, UK. Diffraction data were collected using synchrotron radiation monochromated with silicon(111) to a wavelength of 0.68890 Å. All four data sets were reduced with the use of Bruker SAINT[34] and a multiscan absorption correction applied with the use of SADABS.[35]

The structures were solved by direct methods (SHELXS97) and refined by full-matrix least-squares on F^2 (SHELXL97).[36] Both enantiomers of the chiral C_{90} cages found in isomers I, II, and IV co-exist on the same site due to disorder with respect to a crystallographic mirror plane.

I, Sm@C_2(40)-C_{90}. The C_{90} fullerene cage is disordered with respect to a crystallographic mirror plane that bisects the molecule but is not a symmetry element for the fullerene. Thus, there are two orientations of the C_{90} ball. Due to the crystallographic mirror plane, these two occupancies must sum to 0.5. These orientations were initially refined with variable occupancies and subsequently fixed at the converged values of 0.463 and 0.037, respectively. The major orientation was refined with anisotropic thermal parameters. The minor isomer was pasted in, based on the geometry of the major isomer, with the use of the FRAG command and kept fixed in the final cycles of refinement using isotropic thermal parameters.

There are eight different sites for the Sm atom, which were required to sum to occupancy of 0.5 by the use of free variables and subsequently refined with fixed occupancies. These occupancies are as follow: Sm1, 0.13; Sm2, 0.13; Sm3, 0.08; Sm4, 0.05; Sm5, 0.05; Sm6, 0.04; Sm7, 0.01; and Sm8, 0.01. Only the six sites with highest occupancy were refined with anisotropic thermal parameters; the remaining two sites utilized isotropic thermal parameters.

II, Sm@C_2(42)-C_{90}. The fullerene cage is again bisected by a mirror plane, but in this case all 90 carbon atoms were refined with 0.50 occupancies. There are nine different sites for the Sm atom, which sum to occupancy of 0.5 by the use of free variables. The occupancies for Sm1−Sm9 are 0.112, 0.117, 0.065, 0.045, 0.025, 0.041, 0.056, 0.020, and 0.020, respectively. Only the four sites with highest occupancy were refined with anisotropic thermal parameters; the remaining five sites were kept isotropic.

III, Sm@C_{2v}(46)-C_{90}. Although the fullerene cage has C_{2v} symmetry, none of the symmetry elements of the cage are coincident with those of the crystal. The refinement included two orientations of the fullerene with relative occupancies of 0.88 and 0.12. However, the final difference map indicates that there may be another minor orientation that was not modeled.

The fullerene contains one major site for Sm and seven others at lower occupancy. The occupancies were initially refined and constrained to add to 1.0000 and then fixed. The values are as follow: Sm1, 0.58; Sm2, 0.11; Sm3, 0.08; Sm4, 0.09; Sm5, 0.06; Sm6, 0.03; Sm7, 0.03; and Sm8, 0.02. Anisotropic thermal parameters were used for Sm1−Sm5 only.

IV, Sm@C_2(45)-C_{90}. The C_{90} fullerene cage is disordered with respect to a crystallographic mirror plane that bisects its location. There are two orientations of the C_{90} ball. These orientations were initially refined with variable occupancies and subsequently fixed at the converged values of 0.411(2) and 0.089(2), respectively. The major orientation was refined with anisotropic thermal parameters. The minor isomer was pasted in, based on the geometry of the major isomer, with the use of the FRAG command and kept fixed in the final cycles of refinement using isotropic thermal parameters.

There are six different sites for the Sm atom, which refined to fractional occupancies of 0.292(2), 0.0688(13), 0.0577(12), 0.0375(7), 0.0272(16), and 0.0162(4) for Sm1−Sm6, respectively. Only the three highest occupancy sites were refined with anisotropic thermal parameters; the remaining three were kept isotropic.

Computational Details. Geometries the four isomers of Sm@C_{90}, which were taken from the results of the single-crystal X-ray diffraction, were fully optimized by non-local density functional calculations at the B3LYP level.[37] The effective core potential and basis set developed by Stevens et al. were used for samarium (CEP-31g),[38] and the split-valence 3-21g basis set was used for carbon. All calculations were carried out with the GAUSSIAN 03 program.[39]

■ ASSOCIATED CONTENT

Supporting Information. Complete ref 39; HPLC chromatograms and MS spectra of the purified samples of the four Sm@C_{90} isomers; X-ray crystallographic files in CIF format for Sm@C_2(40)-C_{90}·Ni(OEP)·2chlorobenzene, Sm@C_2(42)-C_{90}·Ni(OEP)·2toluene, Sm@C_2(45)-C_{90}·Ni(OEP)·2toluene, and Sm@C_2(46)-C_{90}·Ni(OEP)·2toluene. This material is available free of charge via the Internet at http://pubs.acs.org.

■ AUTHOR INFORMATION

Corresponding Author
zyliu@cjlu.edu.cn; mmolmstead@ucdavis.edu; albalch@ucdavis.edu

■ ACKNOWLEDGMENT

We thank the U.S. National Science Foundation [Grant CHE-1011760 and CHE-0716843 to A.L.B. and M.M.O.], the U.S. Department of Education for a GAANN fellowship to B.Q.M., the National Natural Science Foundation of China [20971108 to Z.Y.L.], and Natural Science Foundation of Zhejiang Province of China [Y4090430 to Z.M.W.] for support. The Advanced Light Source is supported by the Director, Office of Science, Office of Basic Energy Sciences, of the U.S. Department of Energy under Contract No. DE-AC02-05CH11231.

REFERENCES

(1) Chaur, M. N.; Melin, F.; Ortiz, A. L.; Echegoyen, L. *Angew. Chem. Int. Ed.* **2009**, *48*, 7514–7538.
(2) Dunsch, L; Yang, S. *Small* **2007**, *3*, 1298–1320.
(3) Saunders, M.; Jiménez-Vázquez, H. A.; Cross, R. J.; Poreda, R. J. *Science* **1993**, *259*, 1428–1430.
(4) Kratschmer, W.; Lamb, L. D.; Fostiropoulos, K.; Huffman, D. R. *Nature* **1990**, *347*, 354–358.
(5) Frunzi, M.; Cross, R. J.; Saunders, M. *J. Am. Chem. Soc.* **2007**, *129*, 13343–13346.
(6) Murphy, T. A.; Pawlik, T.; Weidinger, A.; Hohne, M.; Alcala, R.; Spaeth, J. M. *Phys. Rev. Lett.* **1996**, *77*, 1075–1078.
(7) Larsson, J. A.; Greer, J. C.; Harneit, W.; Weidinger, A. *J. Chem. Phys.* **2002**, *116*, 7849–7854.
(8) Harneit, W. *Phys. Rev. A* **2002**, *65*, 032322.
(9) Heath, J. R.; O'Brien, S. C.; Zhang, Q.; Liu, Y.; Curl, R. F.; Tittel, F. K.; Smalley, R. E. *J. Am. Chem. Soc.* **1985**, *107*, 7779–7780.
(10) Chai, Y.; Guo, T.; Jin, C.; Haufler, R. E.; Chibante, L. P. F.; Fure, J.; Wang, L.; Alford, J. M.; Smalley, R. E. *J. Phys. Chem.* **1991**, *95*, 7564–7564.
(11) Okazaki, T.; Lian, Y.; Gu, Z.; Suenaga, K.; Shinohara, H. *Chem. Phys. Lett.* **2000**, *320*, 435–440.
(12) Lian, Y.; Shi, Z.; Zhou, X.; He, X.; Gu, Z. *Chem. Mater.* **2001**, *13*, 39–42.
(13) Liu, J.; Shi, Z.; Gu, Z. *Chem. Asian J.* **2009**, *4*, 1703–1711.
(14) Okazaki, T.; Suenaga, K.; Lian, Y.; Gu, Z.; Shinohara, H. *J. Chem. Phys.* **2000**, *113*, 9593–9597.
(15) Okazaki, T.; Suenaga, K.; Lian, Y.; Gu, Z.; Shinohara, H. *J. Mol. Graphics Modell.* **2001**, *19*, 244–251.
(16) Fowler, P. W.; Manolopoulous, D. E. *An Atlas of Fullerenes*; Clarendon: Oxford, 1995.
(17) Yang, H.; Beavers, C. M.; Wang, Z.; Jiang, A.; Liu, Z.; Jin, H.; Mercado, B. Q.; Olmstead, M. M.; Balch, A. L. *Angew. Chem. Int. Ed.* **2010**, *49*, 886–890.
(18) (a) Achiba, Y.; Kikuchi, K.; Aihara, Y.; Wakabayashi, T.; Miyake, Y.; Kainosho, M. *Mater. Res. Soc. Symp. Proc.* **1995**, *359*, 3–9. (b) Achiba, Y.; Kikuchi, K.; Aihara, Y.; Wakabayashi, T.; Miyake, Y.; Kainosho, M. In *The Chemical Physics of Fullerenes 10 (and 5) Years Later*; Andreoni, W., Ed.; Kluwer: Dordrecht, 1996; p 139.
(19) Yang, H.; Mercado, B. Q.; Jin, H.; Wang, Z.; Jiang, A.; Liu, Z.; Beavers, C. M.; Olmstead, M. M.; Balch, A. L. *Chem. Commun.* 2011, *47*, 2068–2070.
(20) Sun, D.-Y.; Liu, Z.-Y.; Guo, X.-H.; Xu, W.-G.; Liu, S.-Y. *J. Phys. Chem. B* **1997**, *101*, 3927–3930.
(21) Mercado, B. Q.; Jiang, A.; Yang, H.; Wang, Z.; Jin, H.; Liu, Z.; Olmstead, M. M.; Balch, A. L. *Angew. Chem. Int. Ed.* **2009**, *48*, 9114–9116.
(22) Olmstead, M. M.; de Bettencourt-Dias, A.; Stevenson, S.; Dorn, H. C.; Balch, A. L. *J. Am. Chem. Soc.* **2002**, *124*, 4172–4173.
(23) Olmstead, M. M.; Lee, H. M.; Stevenson, S.; Dorn, H. C.; Balch, A. L. *Chem. Commun.* **2002**, 2688–2689.
(24) Mercado, B. Q.; Stuart, M. A.; Mackey, M. A.; Pickens, J. E.; Confait, B. S.; Stevenson, S.; Easterling, M. L.; Valencia, R.; Rodriguez-Fortea, A.; Poblet, J. M.; Olmstead, M. M.; Balch, A. L. *J. Am. Chem. Soc.* **2010**, *132*, 12098–12105.
(25) Stone, A. J.; Wales, D. J. *Chem. Phys. Lett.* **1986**, *128*, 501–503.
(26) Wang, Z.; Yang, H.; Jiang, A.; Liu, Z.; Olmstead, M. M.; Balch, A. L. *Chem. Commun.* **2010**, *46*, 5262–5264.
(27) Mercado, B. Q.; Stuart, M. A.; Mackey, M. A.; Pickens, J. E.; Confait, B. S.; Stevenson, S.; Easterling, M. L.; Valencia, R.; Rodriguez-Fortea, A.; Poblet, J. M.; Olmstead, M. M.; Balch, A. L. *J. Am. Chem. Soc.* **2010**, *132*, 12098–12105.
(28) Kodama, T.; Fujii, R.; Miyake, Y.; Sakaguchi, K.; Nishikawa, H.; Ikemoto, I.; Kikuchi, K.; Achiba, Y. *Chem. Phys. Lett.* **2003**, *377*, 197–200.
(29) Lu, X.; Slanina, Z.; Akasaka, T.; Tsuchiya, T.; Mizorogi, N.; Nagase, S. *J. Am. Chem. Soc.* **2010**, *132*, 5896–5905.
(30) Rodriguez-Fortea, A.; Alegret, N.; Balch, A. L.; Poblet, J. M. *Nature Chem.* **2010**, *2*, 955–961.
(31) Kareev, I. E.; Popov, A. A.; Kuvychko, I. V.; Shustova, N. B.; Lebedkin, S. F.; Bubnov, V. P.; Anderson, O. P.; Seppelt, K.; Strauss, S. H.; Boltalina, O. V. *J. Am. Chem. Soc.* **2008**, *130*, 13471–13489.
(32) Kemnitz, E.; Troyanov, S. I. *Angew. Chem. Int. Ed.* **2009**, *48*, 2584–2587.
(33) Che, Y.; Yang, H.; Wang, Z.; Jin, H.; Liu, Z.; Lu, C.; Zuo, T.; Dorn, H.; Beavers, C. M.; Olmstead, M. M.; Balch, A. L. *Inorg. Chem.* **2009**, *48*, 6004–6010.
(34) *SAINT*; Bruker AXS Inc.: Madison, WI, 2009.
(35) Sheldrick, G. M. *SADABS*; University of Göttingen, Germany, 2008.
(36) Sheldrick, G. M. *Acta Crystallogr.* **2008**, *A64*, 112–122.
(37) (a) Becke, A. D. *Phys. Rev. A* **1988**, *38*, 3098–3100. (b) Lee, C.; Yang, W.; Parr, R. G. *Phys. Rev. B* **1988**, *37*, 785–789.
(38) Stevens, W.; Basch, H.; Krauss, J. *J. Chem. Phys.* **1984**, *81*, 6026–6033.
(39) Frisch, M. J.; *et al. Gaussian 03*, Revision C.02; Gaussian Inc.: Wallingford, CT, 2004